From quarry by-products to a zeolites-based Zn fertilizer with increased resistance to rain leaching

Galamini Giulio [a], Daniele Malferrari [a,c,*], Altimari Fabiana [b], Orlandi Silvia [b], Barbieri Luisa [b,c]

[a] *Department of Chemical and Geological Sciences – University of Modena and Reggio Emilia, Via G. Campi 103, 41125, Modena, Italy*
[b] *Department of Engineering "Enzo Ferrari" – University of Modena and Reggio Emilia, Via P. Vivarelli 10, 41125, Modena, Italy*
[c] *BIOGEST-SITEIA, Piazzale Europa 1a, 42124, Reggio Emilia, Italy*

ARTICLE INFO

ABSTRACT

In the face of an extensive literature on the use of zeolites for the removal of metals from water for environmental purposes, it is seldom considered that some metals are also essential nutrients for life and that zeolites could be profitably used to dose their release. Among these, Zn is a key micronutrient, and when its demand by crop is not fully balanced by adequate accessibility, fertilization must be provided using Zn salts that can be, however, easily leached and partly wasted in the environment.

In an attempt to solve this critical problem, a new controlled-release formulation of Zn using zeolite-containing geomaterials was designed, prepared, characterized, and tested by applying a sequential, multi-method approach. Different formulations were trialed, and the most effective included 30 wt% pumice by-product and 70 wt% clinoptilolite-rich zeolitized tuff, with about 20 mg/g of exchangeable Zn^{2+}. The enrichment process reached equilibrium after about 8 h, a timing well-tuned with technology transfer. Desorption kinetic tests in a weekly acid environment revealed gradual Zn release, with about 4.28 wt% released after 6 h. When tested as a foliar fertilizer on *Vitis vinifera*, this formulation demonstrated superior resistance to leaching under simulated rainfall conditions compared to conventional $ZnSO_4 \cdot 6H_2O$ fertilizer, maintaining the initial level of Zn (130 mg/kg of dry leaves), while about 22 % of the Zn applied with $ZnSO_4 \cdot 6H_2O$ was loss. This outcome was plausibly due to mineral particle adhesion to leaf. Preliminary cost estimates suggest that the product designed here can be placed in the market with competitive sales prices.

1. Introduction

To supply fertilizers to the aerial part of plants, the use of cation-exchanging microporous materials could be a viable option [1–6]. Among them, zeolites are very promising geomaterials [7–11]. In fact, zeolites are characterized by properties such as high and selective cation–exchange capacity (CEC), reversible hydration and molecular sieving, which give them a high agronomic value [12–14]. This success is confirmed by several studies and applications regarding their use as soil amendments [15–28], for nutrient recovery from wastewaters and livestock manure [26,29–35] and, more recently, as corroborants for foliar treatments, also due to their persistence on leaf surfaces when applied in micronized form [17,36–44].

Although recent studies show that zeolites synthesized from wastes such as fly and bottom ash can be used in a variety of application contexts [45–47], almost just volcanic tuffs are currently used in agriculture

[48]. Volcanic tuffs are rocks that may contain up to 70–80 wt% of zeolitic species such as clinoptilolite, mordenite, phillipsite and chabazite in varying amounts depending on the genetic conditions and geological history of the area. It is important to emphasize that using zeolitized tuffs in agriculture does not necessarily involve the opening of new quarries, but rather the exploitation of by–products from already existing ones. In fact, in the past (and largely even today), zeolitized tuffs were used to obtain natural stone for construction; over the years, considerable amounts of zeolite-rich scraps have accumulated (Fig. SOM-1 in Supplementary Online Material, SOM here after, in Appendix A) that can be profitably used in various large-scale applications [17,22,23,26], becoming a core business for many quarries.

On the other hand, there are more problematic quarrying by-products, such as those resulting from the mining and processing of pumices and lapilli, highly porous rocks originating from explosive volcanic events. Nevertheless, both pumice and lapillus, like tuffs, may

contain nonnegligible amounts of zeolitic species (up to 15 wt%), possibly making these geomaterials effective cation exchangers. Unfortunately, according to regulations currently in force in Italy [49], and indirectly applied in other nations as well, only geomaterials that contain at least 50 wt% of zeolitic species, whether or not they are by–products, can be classified and traded as soil improvers, which are the major source of consumption of these by-products in agriculture. Therefore, finding additional ways to use geomaterials with modest zeolitic content is undoubtedly a timely challenge, with not only environmental, but also managerial and economic implications, considering that the mining sector produces more than 100 billion tons of solid waste per year globally [50].

In the face of numerous studies involving zeolites in Zn removal for various environmental application, only very few researches have considered them as an efficient geomaterial for Zn fertilization in soil or plant leaves [51] or to modelling the heavy metals, including Zn, mobility in zeolite-amended soils, with implication also on their bioavailability [52,53]. Zn is a fundamental micronutrient for humans, being responsible of catalytic, structural and regulatory functions in mammalians [54]. About 33 % of the Zn ingested is effectively absorbed in the small intestine, where it is then transported to the liver, and finally to other tissues via the systemic circulation [55]. Cellular Zn pools are then regulated by the influx or release from intracellular stores of Zn or supplied by either metallothioneins (proteins that bind Zn and act as an intracellular reservoir), or heavy-metal ATPases (enzymes that control Zn in cytosol using the energy of adenosine triphosphate) [56]. The importance of Zn for human body is evidenced by the many roles of Zn finger proteins, that control the expression of growth-related genes, immune response mediators, and steroid receptors [57]. Despite this, Zn deficiency is a growing threat, especially in poor and developing countries, often resulting in increased susceptibility to infections, reduced physical power, growth retardation, as well as neurobehavioral impairments in children [58–61]. The main reasons for low dietary intake are poor levels of bioaccessible Zn in agricultural soils (about 50 % show inadequate levels of Zn) and non–diversified diets based on cereals and cereal-based products [62–64]. The latter, is indeed a common feature inherited from earliest days of agriculture, around 9 K–years ago, when only a few species of cereals (wheat, rice and maize) were selected for cultivation [65]. Because Zn, as well as other essential micronutrients, increase its concentration within specific trophic levels along terrestrial food webs (biomagnification), significantly higher levels of Zn are present in animal products and meat than in cereals [66]; consequently, low or null consumption of meat in developing countries is among the causes of Zn deficiencies and related pathological disorders [60].

Beyond this, there are other aspects not strictly related to food safety and accessibility, but still relevant to the economies of many countries. In fact, an adequate supply of Zn is also crucial in horticulture and viticulture, as it contributes to plant health [67–70]. For plants, Zn is an essential component of Zn-binding proteins with structural functions. It is involved in transcription, translation, photosynthesis, and the metabolism of reactive oxygen species [71]. Zn is also important for plant–pathogen and pest interactions [72]. Indeed, increased levels have been associated with heightened immune system response and resistance to pathogenic infections, while deficiencies have been related with increase susceptibility to fungal diseases [73,74]. Deficiency symptoms include chlorosis, reduced growth and yield, and reduced micronutrients in cereals grains [71]. Radial transport of Zn to the xylem (and thus to the shoots) occurs through two main pathways, namely the symplastic and apoplastic. The former transports Zn (as well as sugars and other molecules) between cells within the cytoplasmic continuum of root cells, the latter through extracellular spaces called apoplasts, where specific barriers (e.g., the Casparian stripe) serve to control nutrient fluxes [71,75]. In all cases, the presence of Zn in bioavailable form is critical.

Stimulating Zn bioaccumulation in plants (biofortication) could be a valid response in contexts where crop demands for Zn is not fully balanced by adequate Zn accessibility from the soil [76–80]. Nevertheless, the efficacy of Zn fertilization in soils is often limited by several reasons, including, the high solubility and rapid leaching of mineral Zn fertilizers, the possible sequestration through cation exchange reactions with clay minerals and the soil organic matter (formation of non-bioavailable organometallic complexes), and limited translocation from root systems to edible parts of plants [81–89]. In addition, its mobility can be affected, although to a lesser extent than other metals, just by soil amendment actions with zeolites [52] or other organic and inorganic amendments [90]. For these reasons, Zn foliar application has gained momentum as an alternative or supplementary strategy to soil application [91–93]. Moreover, particularly promising scientific outcomes [94–96] recently demonstrated with ^{65}Zn isotopic tracing, efficient translocation of Zn from wheat leaves to grains, further validating foliar fertilization as a preferential technique. The choice of one or the other strategy should be however weighed against the site-specific characteristics of the soil [89], the crop [76,80,97], and the type of Zn-based fertilizer [98].

Based on these premises, this research aims to prepare a new controlled-release Zn foliar fertilizer [99] composed of a mixture of zeolites-containing quarry by-products with the purpose of reducing environmental impacts and quarry costs. This formulation should release Zn gradually over a longer period than a conventional fertilizer and, therefore, provide plants with a steady and sustained supply of Zn for growth while minimizing nutrient loss through leaching. The possible occurrence of different zeolitic species in the various geomaterials used, could also provide advantages in terms of differential release of Zn (i.e., kinetic), as each zeolitic species reacts differently depending on its crystal chemistry [100–102]. More specifically, Zn adsorption and desorption and cations diffusivity were investigated in mixtures with varying amount of a clinoptilolite-rich zeolitized tuff, pumice and lapillus scraps. The most promising formulation was then tested as foliar fertilizer on *Vitis vinifera* to evaluate its resistance to simulated rain leaching with respect to a commonly used Zn fertilizer ($ZnSO_4 \cdot 6H_2O$). A preliminary cost-benefit analysis was performed as well.

2. Instruments, materials and methods

2.1. Analytical instruments

Geomaterials were characterized with a consolidated multi–analytical protocol [103,104], encompassing particle size analysis, surface areas measurement with the multi-point Brunauer–Emmett–-Teller (BET) method, X-ray powder diffraction (XRPD), X–ray fluorescence (XRF), scanning electron microscopy equipped with an energy dispersive X–ray detector (SEM-EDX) and elemental analyses (EA) to quantify the carbon and nitrogen contents, the latter used to calculate the CEC in the geomaterials saturated with $[NH_4]^+$. Inductively coupled plasma optical emission spectroscopy (ICP–OES) was used for measuring the dissolved cations (Zn^{2+}, Al^{3+}, Na^+, Mg^{2+}, K^+, Ca^{2+}) in liquid samples. Detailed description of instruments and experimental set up is reported in the SOM–1.

2.2. Geomaterials

The geomaterials used (section 3.1) are a clinoptilolite-rich zeolitized tuff (ZT), pumice (PU) and lapillus (LA) from Bono (Sassari, Sardinia, Italy), Riserva Muraccio (Tessennano, Viterbo, central Italy) and Monte Cellere (Cellere, Viterbo, central Italy) quarries, respectively. The analytical methods employed for their characterization are described in SOM–1 and SOM–2. More information on the properties and applications of geomaterials like those used in this study are described in the literature [105–107].

2.3. Formulations design and preparation

In the following, Zn and Zn^{2+} will be used to refer to the metal in the broad sense or the exchangeable cation, respectively. As indicated in the labels of a wide range of commercial products and also in the literature [108–110], the recommended doses of Zn for foliar applications range between 200 and 300 g/ha, depending on various factors such as soil conditions and specific nutritional requirements of crops. Therefore, a formulation containing about 20 mg of exchangeable Zn^{2+} per g of product (equivalent to 61.2 mEq of Zn^{2+} per 100 g) was foreseen. Under these conditions, the amount of product used would be about 10–15 kg/ha, paralleling the dosage usually employed in foliar treatments with natural powdered corroborants.

Based on the results after described in section 3, four different formulations were prepared, identified hereafter as $ZT^{70}PU^{30}$, $ZT^{70}LA^{30}$, $ZT^{85}PU^{15}$ and $ZT^{85}LA^{15}$ composed of 70 or 85 wt% of ZT and 30 or 15 wt% of PU or LA, respectively. Preparation was done by simultaneously grinding appropriate amounts of each geomaterial in an agate mill until a micronized powder was obtained as indicated by the particle size analyses (Figs. SOM-2-SOM-5).

2.4 The adsorption of Zn^{2+} by ZT at equilibrium and non–equilibrium conditions

The CEC of a zeolite depends not only on its crystal chemistry and exchangeable cations, but also on several other parameters, including particle size, interaction time, and the solid/solution ratio [100–102]. Therefore, once fixed the particle size, the minimum contact time required to obtain a near–equilibrium condition, and the optimum solid/solution ratio were accessed by kinetic (time dependent) and equilibrium (equilibrium concentration dependent) adsorption tests, respectively, as detailed in SOM–3. Although cation exchange may be boosted by temperature, it is still a spontaneous reaction and room temperature (20 °C) was used in this research to avoid any waste of energy.

2.5. Preparation of Zn^{2+}–enriched formulations and release tests

The four formulations ($ZT^{70}PU^{30}$, $ZT^{70}LA^{30}$, $ZT^{85}PU^{15}$ and $ZT^{85}LA^{15}$) were enriched in Zn^{2+}, according to the results of adsorption kinetic tests. The amount of adsorbed Zn^{2+} was checked through ICP–OES after conventional nitric–hydrofluoric digestion. Each formulation was investigated for Zn^{2+} desorption kinetic in a weakly acid environment, simulating common rain pH [111], and compared with ZT. Details about Zn^{2+} loading and desorption kinetic batches are reported in SOM–4.

2.6. Residence test on Vitis vinifera after a simulated rain event

$ZT^{70}PU^{30}$ formulation was selected as the most promising option (see section 3.4 for details) and therefore further investigated as foliar treatment on *Vitis vinifera* (Trebbiano Romagnolo cultivar). The test was performed by a professional agronomist in a greenhouse (Valsamoggia, Bologna, north Italy) and included a positive control (plant fertilized with $ZnSO_4 \cdot 6H_2O$, as conventional fertilizer) and a negative one (no treatment) to asses background Zn. Briefly, more details are given in SOM-5, 15 plants were sprayed, 5 with the formulation ($ZT^{70}PU^{30}$), 5 with $ZnSO_4 \cdot 6H_2O$ solution (positive control) and 5 with tap water (control). Each plant received 3 treatments, each 48 h apart, which provided, a total of 20 mg Zn per plant (regardless of the source of the metal, i.e., the $ZT^{70}PU^{30}$ or $ZnSO_4 \cdot 6H_2O$). The aim was to verify the persistence of Zn (both bioaccessible and its total amounts) on the leaves, before and after a simulated rain event. To achieve this information, sequential extractions were applied (SOM-5). The leachable fraction was evaluated in water extracts, while the fraction resistant to the leaching was measured in subsequent extracts of concentrated HNO_3. The former for the purpose of measuring leachable Zn from rain,

the latter the Zn absorbed by leaves or present in the formulation remaining on the leaves. A further check followed a more conventional procedure by analysing total Zn in leaves ash.

Significant differences ($p < 0.05$) were obtained with ANOVA and Tukey's HSD tests, that were used for normally distributed, homoscedastic populations (as resulted from Shapiro–Wilk and Bartlett's tests), whereas Kruskal–Wallis was used for non–normally distributed, non––homoscedastic data. Statistical analyses were performed with R Studio [112], using MASS [113] and Agricolae [114] packages.

3. Results and discussion

3.1. Geomaterials characterization

The XRPD pattern of the considered geomaterials are reported in Fig. 1. From a strictly qualitative point of view, XRPD results indicate that mica/illite, plagioclase, quartz and sanidine are present in all samples in varying amounts.

ZT is characterized by a significantly high amount of clinoptilolite (Table 1), with Na^+, Ca^{2+} and Mg^{2+} as the main exchange cations, as suggested by CEC and chemical analyses (Table 1, Section 3.3). Chabazite and analcime are the zeolitic species found in PU and LA, respectively (Table 1), but in lower amounts than in ZT, in accordance with the lower CEC of these two geomaterials (Table 1), a parameter closely related to the amount of zeolitic species. Hematite and pyroxene are also present in LA, in agreement with the higher Fe and Mg content in this sample compared to ZT and PU. All samples are also characterized by a significant presence of undetectable material in X diffraction (likely
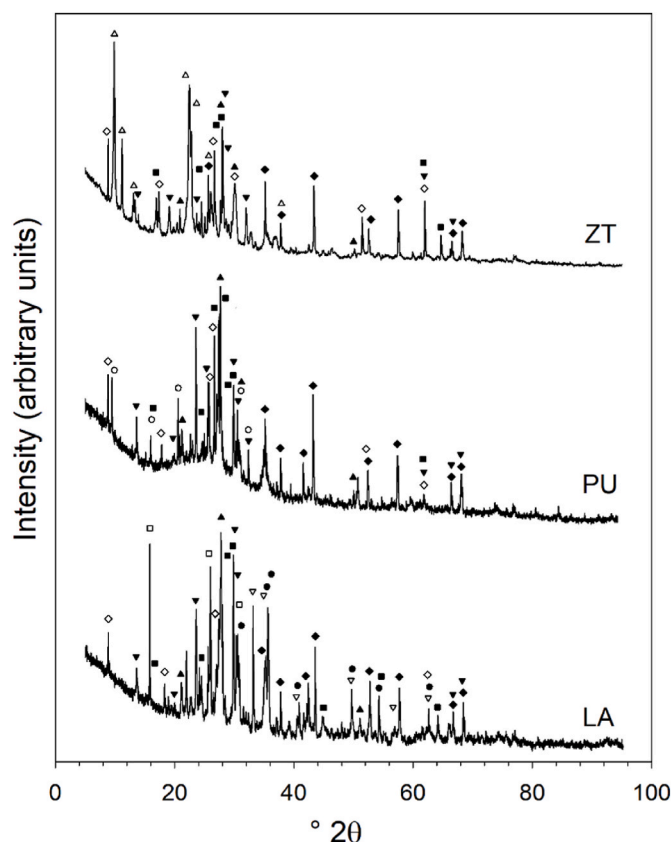

Fig. 1. XRPD patterns of ZT, PU and LA. Symbols identify the main peaks of the detected phases (Table 1) and of the internal standard NIST SRM 676a (alumina powder, corundum structure – see SOM 1.1). Open symbols: square, analcime; circle, chabazite; triangle up, clinoptilolite; triangle down, hematite, diamond, mica/illite. Filled symbols: square, plagioclase; circle, pyroxene; triangle up, quartz; triangle down, sanidine, diamond, corundum (standard).

amorphous), however, typical of geomaterials such as these originating from explosive volcanic events. This feature is also well evidenced by the increase in background signal [115] that is observed for all samples between about 20 and 30 °2θ (Fig. 1); in fact, this increase is best evident in the PU sample, which is the one characterized by the greatest amount of amorphous (Table 1).

In agreement with its mineralogical composition (about 64 wt% of clinoptilolite) and as found for other similar geomaterials (clinoptilolite-rich tuffs) recently described in the literature [118–122] ZT has a specific surface area of 22.838 ± 0.238 m^2/g. This value is close to that of PU (18.005 ± 0.099 m^2/g) and significantly higher than that of LA (2.106 ± 0.023 m^2/g). Although zeolitic tuffs generally have a slightly higher surface area than pumices due to their crystalline and microporous structure, a direct comparison between these different materials is not possible because of the different geological context of origin and the different processing undergone [123].

3.2. Characterization of Zn^{2+} adsorption by the ZT

The Zn^{2+} adsorption equilibrium test on ZT (see SOM–3.1 for experimental detail) showed a peculiar C_e–q_e plot, where C_e (equilibrium concentration of Zn^{2+} in solution, mg/L) and q_e (Zn^{2+} adsorption capacity at equilibrium, mg/g) were indirectly related (Fig. 2A). Inverse q_e to C_e trends are not possible in cation exchange, as they represent a condition where the higher the mass/volume ratio, the more exchange occur per unit mass. Nevertheless, inverse q_e to C_e correlations likely represent a system where fractions of Zn^{2+} precipitated as low soluble salt. SEM–EDX analysis (Fig. 3) carried out on ZT powder derived from batch ≥6 % w/v (SOM 3.1) effectively revealed the occurrence of domains with significative Zn amounts, up to localized 70 wt%. Since ZT was washed several times with Milli–Q water after the exchange with Zn^{2+}, and EDX spectra (Fig. 3) did not reveal sulfur–related signals, the occurrence of residual $ZnSO_4 \cdot 6H_2O$ is not plausible. Considering that the tCEC of the ZT was 159 mEq/100g (Table 1), the maximum adsorbable Zn^{2+} should not exceed 5.2 wt%. Values significantly higher than 5.2 wt % (also considering the semiquantitative outreach of EDX measurements) are therefore not explainable with adsorption/exchange reactions, supporting instead the occurrence of Zn precipitate (condition

represented by red dots in Fig. 2).

Curves in Fig. 2A shows that the precipitation of Zn phases was ZT dose–dependent. The addition of zeolites to a solution can indeed apport significant differences in chemical properties, not only in terms of cation exchange, but also concerning pH. More specifically, zeolites may significantly increase the pH of soils [52] and solutions, possibly favouring the precipitation of metal oxide and hydroxide [124]. Paralleling the procedure described in SOM 3.1, a test was performed for evaluating the pH variation starting from a 0.1 M $ZnSO_4 \cdot 6H_2O$ solution, in contact with different doses of ZT, with solid/liquid ratios ranging from 1 to 16 % (w/v). Samples were mixed at 400 rpm in closed PVF flasks for 24 h, then pH was measured (Fig. 2B). The initial pH was 4.8, slightly lower than the theorical value (5.0) calculated with Equation (1), considering $pK_{a1} = 9.05$ and $C(s) = 0.1$ M [125], because of the addition of a few drops of HNO_3, used to facilitate the solubilization of $ZnSO_4 \cdot 6H_2O$.

$$pH = 0.5 pK_{a1} - 0.5 \log (C_s) \qquad (1)$$

Once in contact with ZT, pH linearly increased with ZT dosage, to a maximum of 7.8 (reached at 16 % w/v). The condition that first revealed Zn precipitates in SEM–EDX analysis (6 % w/v) showed a pH of 5.8. It is therefore likely that pH change by zeolites concurred in the precipitation of Zn phases [126]. In fact, Fig. 3A shows a grain of ZT material after $ZnSO_4 \cdot 6H_2O$ batch, surrounded by smaller tabular or plate–shaped precipitates and the regions within red dashed lines in Fig. 3B, revealed Zn concentrations greater than 20 wt%.

3.3. Cation exchange kinetic of ZT during Zn^{2+} adsorption

Zn^{2+} adsorption kinetic measurements were performed as described in SOM–3.2. The cations released by ZT during Zn^{2+} adsorption are reported in Table 1. Equilibrium desorption capacities (q_e, measured at 28 h) for Na^+, Ca^{2+}, K^+ and Mg^{2+} indicate an aCEC of 83.4 mEq/100g (Fig. 4A; Table 1). As expected, this value was significantly lower than the tCEC measured using $[NH_4]^+$ as the exchange cation (159 mEq/100g, Table 1) because of the lower affinity of clinoptilolite towards Zn^{2+} compared to $[NH_4]^+$ [102,127]. However, with respect to ZT, the value of 83.4 mEq/100g for Zn^{2+} largely meets the target required for a

Table 1
Mineralogical (weight %) and chemical (oxide weight %) composition of ZT, PU and LA. In the mineralogical analyses (left) the standard deviation σ_Q (values in parenthesis) of the weight percentage Q of each phase was calculated using the values obtained in the output file after the quantitative refinement by GSAS software, and the formula $\sigma_Q = \{[(\sigma_a/a)^2 + (\sigma_b/b)^2]^{1/2}\}$ Q [116], where a and b are the two variables most affecting Q values and refer, respectively, to the weight fraction of the phase and the internal standard, whereas σ_a and σ_b are their standard deviations; "Amorphous" may also include very low-amount minor phases non detected through XRPD. In chemical analysis (right) the LOI (Loss On Ignition) is the weight loss (%) at 1050 °C. CEC are reported in mEq/100g as tCEC (theoretical CEC, cations exchange with $[NH_4]^+$ and aCEC (apparent CEC, cations exchange with Zn^{2+}), both as defined in Inglezakis (2005) [117] and detailed in SOM-2. Counterions are referred to aCEC and were measured only for ZT being the main component of the formulations described in section 3.3.

	ZT	PU	LA		ZT	PU	LA
Analcime	–	–	7.5(5)	LOI	12.7	4.30	1.07
Chabazite	–	12.4(2)	–	SiO_2	64.2	60.5	49.8
Clinoptilolite	63.7(8)	–	–	Al_2O_3	12.2	17.9	17.5
Hematite	–	–	7.8(3)	Fe_2O_3	2.85	3.23	9.33
Mica/Illite	2.7(2)	4.7(1)	1.8(6)	MnO	0.0821	0.143	0.140
Plagioclase	6.3(2)	3.9(2)	22.1(1)	MgO	1.47	0.946	3.47
Piroxene	–	–	14.6(9)	Na_2O	1.84	2.73	4.37
Quartz	2.0(5)	2.3(1)	0.80(7)	TiO_2	0.298	0.393	1.08
Sanidine	2.9(3)	24.7(3)	7.6(6)	K_2O	1.87	7.55	3.36
Amorphous	22.4(9)	52.1(5)	37.8(8)	P_2O_5	0.0611	0.0781	0.346
				CaO	2.38	2.42	8.99
χ^2	4.428	3.383	5.216	C	0.30	0.10	0.05
R_p	0.0550	0.0524	0.0924				
R_{wp}	0.0805	0.0738	0.0916	tCEC	159	22.3	8.93
				aCEC	83.4 of which:		
				Na^+	52.0		
				Ca^{2+}	15.3		
				K^+	4.55		
				Mg^{2+}	11.5		
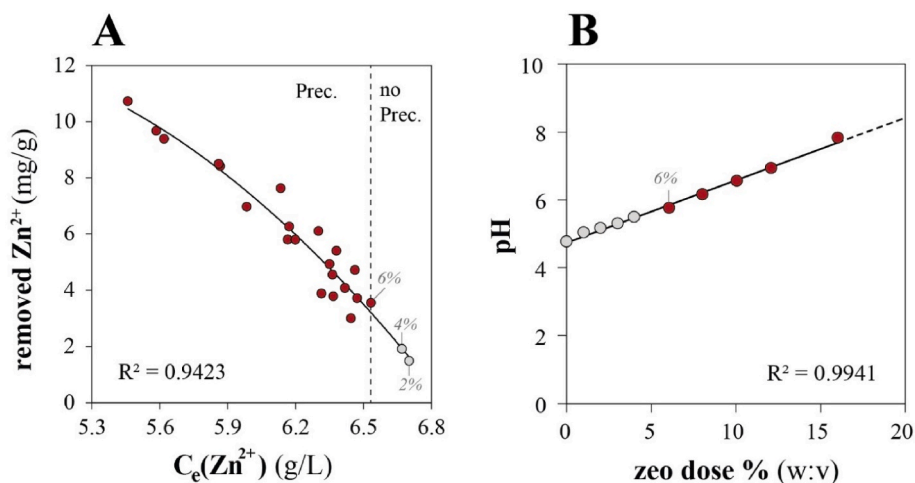
Fig. 2. Zn^{2+} adsorption equilibrium test. A) Removed Zn^{2+} at equilibrium per g of ZT, respect to residual Zn^{2+} dissolved. 2nd grade polynomial and R^2 are shown. The dotted vertical line separates the region where Zn precipitates occurred (ZT ≥ 6 % w/v, at the left) with the one where no precipitates have been observed (ZT < 6 % w/v, at the right); B) pH effect of different w/v ratios of ZT in $ZnSO_4 \cdot 6H_2O$ 0.1M solution. Percentages (%) are intended as w/v (g of ZT/100 ml).
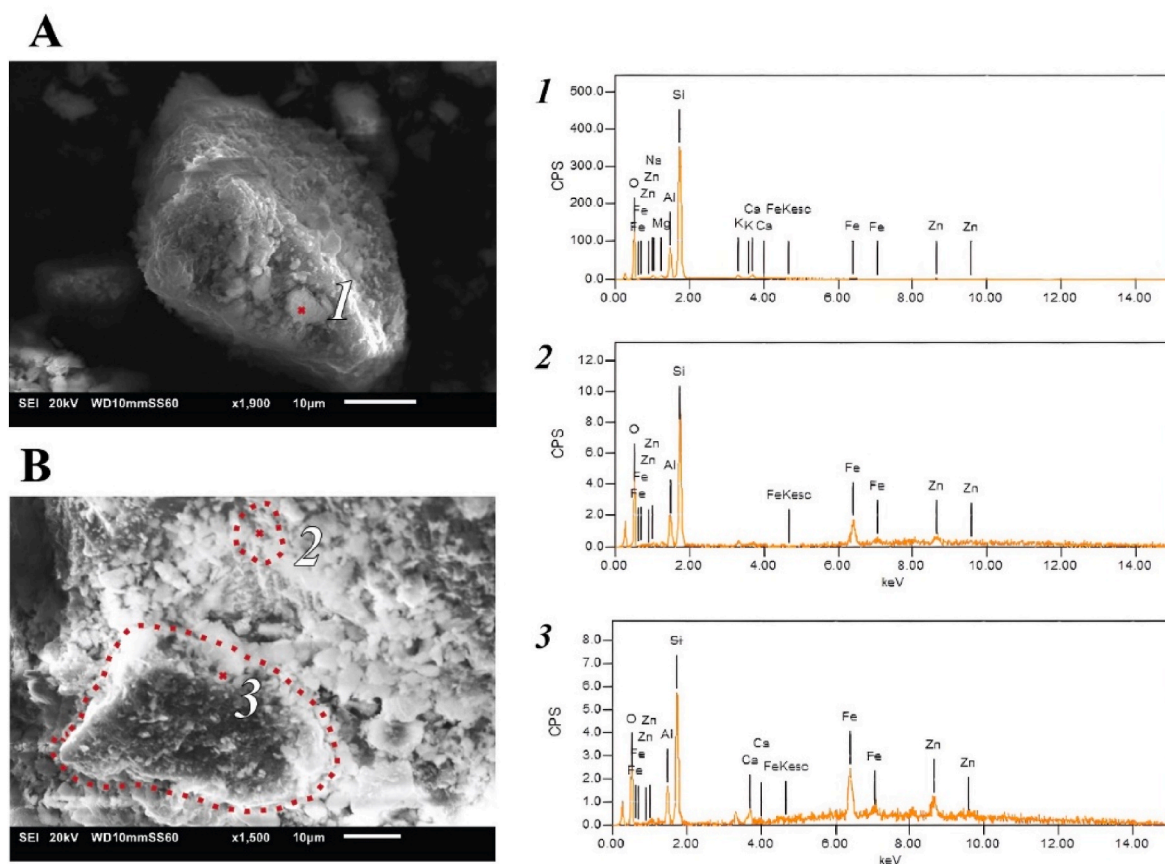
**Fig. 3.** SEM–EDX of the ZT treated with $ZnSO_4 \cdot 6H_2O$ 0.1M solution (at 6 % w/v batch). A) A grain surrounded by smaller tabular crystals; B) particular of a region with high Zn content (>20 wt%), highlighted by red dotted lines. On the right the EDX spectra of measurements point 1, 2 and 3 indicated in Figs. A and B.

Zn-fertilizer (61.2 mEq/100g, section 2.3).

For each measured q(t) (time-dependent desorption capacities of exchangeable cations), the fractional uptake F(t) was calculated as F(t) = q(t)/q_e [128], where F(t) represents the closeness of the system to equilibrium. Indeed, in kinetic investigations it should be avoided to use data too close to equilibrium [128], therefore, only data with F(t) < 0.85 were considered. The F(t) values calculated for each exchangeable cation are shown in Fig. 4B. The ZT released monovalent cations (Na^+ and K^+) quicker than bivalent ones (Ca^{2+} and Mg^{2+}) as near equilibrium conditions (F(t) ≥ 0.85) was reached for Na^+ and K^+ after about 30 min of contact, while Ca^{2+} and Mg^{2+} showed F(t) ≥ 0.85 after about 4 h of contact. Cations with higher hydration energy, as Mg^{2+} and Ca^{2+}, present slower exchange kinetic than cations with lower hydration energy, as Na^+ and K^+; furthermore, zeolites with high SiO_2/Al_2O_3 ratio as clinoptilolite show increase affinity for monovalent exchangeable cations [102,127,129].
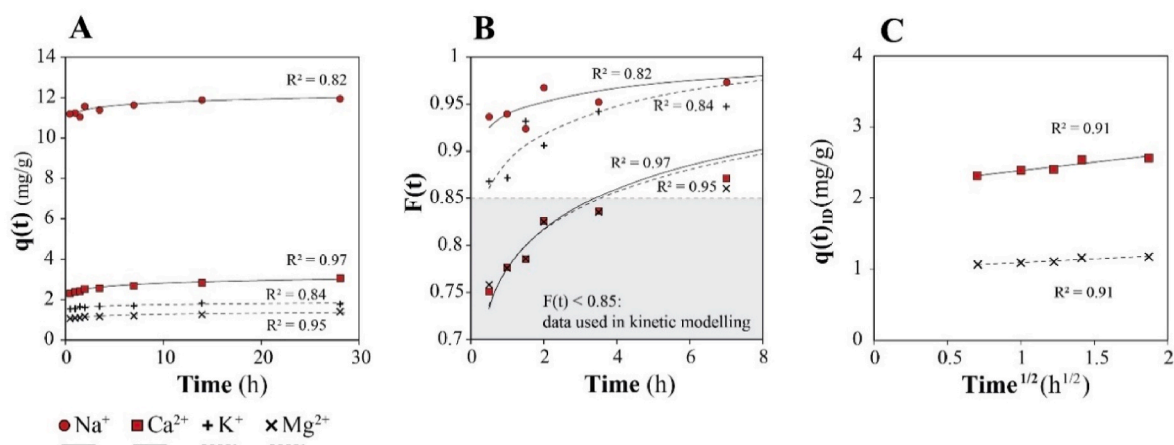
Fig. 4. Desorption kinetic of Na^+, Ca^{2+}, K^+ and Mg^{2+} by the ZT in a $ZnSO_4 \cdot 6H_2O$ 0.1 M batch. A) q(t) (mg/g) vs Time (h); B) F(t) vs Time (h). The grey region represents F(t) < 0.85, therefore, the data contained were not considered in kinetic modelling. The curves in A and B are logarithmic regressions with R^2 indicated. C) Intraparticle Diffusion (ID) model for Ca^{2+} and Mg^{2+} and relative R^2 [130].

Kinetic modelling was performed for Ca^{2+} and Mg^{2+} being that only these cations provided data with F(t) < 0.85. The Pseudo–Second Order (PSO) [131] showed good correlation with experimental data (Equation (2)):

$$q(t) = \frac{q_e^2 k_2 t}{1 + q_e k_2 t} \quad (2)$$

where q(t) (mg/g) is the time-dependent adsorption/desorption capacity, q_e (mg/g) is the equilibrium adsorption/desorption capacity, k_2 is the PSO rate constant (g/mg h) and t is time (h). The PSO showed an optimal correlation with experimental data ($R^2 > 0.999$), however not all the assumptions were plausibly met [132], briefly: (i) adsorption is reaction–controlled, (ii) liquid concentration is constant, and (iii) no desorption occur. To exclude spurious correlations, it has been pointed out to check the distribution of standardized residuals [132] that, in this case, were not homogeneously distributed, finally confirming the inconsistency of the PSO model. Being that ZT and, particularly zeolites are microporous materials, cations diffusivity could be relevant [133]. The Weber–Morris Intraparticle diffusion model was therefore investigated (Equation (3)):

$$q(t) = k_{ID} t^{0.5} + C \quad (3)$$

where K_{ID} is the diffusion rate constant and C (mg/g) is related with the diffusivity in the boundary layer [134]. The occurrence of multiphase adsorption could be verified in the q(t) vs $t^{1/2}$ plot (Fig. 4C), if multiple lines are present. In the case, the first step (line with intercept C = 0) represents external diffusion, followed by diffusivity–controlled adsorption [135]. Sole intraparticle diffusion occurs instead when a single line is present, intersecting the origin at C = 0, with K_{ID} as slope.

The intercept C is also related with the thickness of the boundary layer (physisorption), whereas monolayer condition (as the case of chemisorption and cation exchange) is related with C values near zero [134]. In this case, starting from 30 min of contact, C was 2.15 and 0.993 mg/g for Ca^{2+} and Mg^{2+}, respectively (Fig. 4C), while k_{ID} was 0.238 and 0.101 mg/g h^{-1}, suggesting that the diffusion of the exchanged species through extra–framework spaces of zeolite crystals toward the external environment did not significantly limit Zn^{2+} adsorption, at least starting from 30 min of contact, also in agreement with its surface area. The ZT is a micronized material, therefore the micropores where highly exposed to the external environment facilitating cations diffusivity both outside and inside (Zn^{2+}) the zeolitic channels. This aspect was likely particularly relevant for monovalent exchangeable cations, where the most present one (Na^+) showed an F(t) = 0.94 just after 30 min of contact, suggesting no significant

limitations in its diffusivity during Zn^{2+} exchange.

3.4. Zn^{2+} enrichment of the formulations and released in simulated rain water

In agreement with the assumptions outlined in section 2.3, and considering the results of sections 3.2 and 3.3, four formulations were prepared by mixing different amounts of ZT with PU and LA by-products, reducing the amount of ZT to a maximum of 30 %, therefore sufficient to ensure a CEC approximately equal to the fixed target (61.2 mEq Zn^{2+} per 100 g). The four mixtures were labelled as defined in section 2.3 and Table 2 where is also reported the amount of Zn^{2+} adsorbed after the enrichment (SOM–4).

The minor increase of Zn content in the formulations compared to the values that could be calculated from Zn–exchanged ZT (namely, −30 % ZT → 58.4 mEq/100g, and −15 % ZT → 69.5 mEq/100g) is consistent with the contribution to cation exchange of zeolites occurring in LA and, especially, PU (Table 1). Equilibrium was almost reached after 8 h, a promising timeline for technology transfer.

The interaction with simulated rain water (SOM–4) shows a gradual Zn^{2+} release (Fig. 5) for all the formulations; the total amounts of metal released remained low even after a contact time of 6 h (Table 2). The initial fast release recorded at 30 min was plausibly due to exchange process occurred in the outermost part of the zeolitic channels, that was also facilitated by the reduced grain size. This peak is more pronounced (higher release) in the $ZT^{70}PU^{30}$ formulation, even compared to the pure ZT, plausibly related to the presence in PU of chabazite (Table 1) which has higher CEC and faster release than clinoptilolite [15,136,137], the zeolitic specie occurring in ZT, rather than their surface area presenting similar values. The chabazite contained in PU (i.e., in the $ZT^{70}PU^{30}$ formulation) therefore increased the initial release rate of Zn^{2+}; subsequently, at higher times the release curves of $ZT^{70}PU^{30}$ and ZT tend to converge, due to the higher abundance of zeolite (and exchangeable Zn^{2+}) in ZT than $ZT^{70}PU^{30}$. Similar considerations apply also to

Table 2
Zn^{2+} contained in enriched formulations (left) and percentages released after 6 h of contact with acidified water (HNO_3, pH 5.5) to simulate rain water (right). Data for pure ZT (label ZT^{100}) are also reported for ease of comparison.

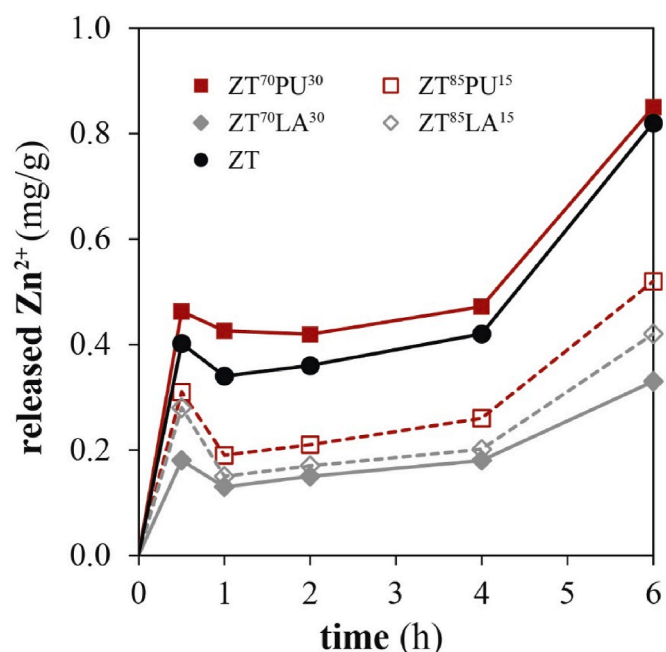|	mg/g (mEq/100g)	Release 6h (%)
$ZT^{70}PU^{30}$	19.86 (60.8)	4.28
$ZT^{70}LA^{30}$	20.16 (61.7)	1.63
$ZT^{85}PU^{15}$	23.00 (70.4)	2.26
$ZT^{85}LA^{15}$	22.70 (69.5)	1.85
ZT^{100}	26.71 (81.7)	3.07

Fig. 5. Release kinetic of the formulation ZT^{70}PU^{30}, ZT^{70}LA^{30}, ZT^{85}PU^{15} and ZT^{85}LA^{15} compared to pure ZT.

ZT^{85}PU^{15} and ZT^{85}LA^{15}, although the difference is less pronounced due to the higher amount of zeolite (clinoptilolite) compared to ZT^{70}PU^{30}. ZT^{70}LA^{30} shows instead slower kinetics and lower release due to lower zeolite content, as the LA provided only minor amounts of analcime and also has a smaller surface area than ZT, which could limit cation diffusivity. For all the treatments, between 30 and 60 min the released Zn^{2+}

slightly dropped, indicating that re-adsorption and/or precipitation occurred, however, Zn^{2+} continue to be slowly released over time.

3.5. Residence of ZT^{70}PU^{30} formulation on plant leaves following simulated rain event

For the reasons given in section 3.4, ZT^{70}PU^{30} was considered the most suitable formulation among the four tested. Therefore, it was used to perform residence tests on *Vitis vinifera* leaves, in comparison with conventional ZnSO$_4$·6H$_2$O foliar fertilizer (see sections 2.6 and SOM-5 for further details).

The amount of Zn in the negative control was significantly lower (about −87 % less) than in the treated leaves and, as expected, no substantial differences were observed before and after the simulated rain.

Before the rain event (PRE rain columns in Fig. 6A), regarding total Zn, no differences were observed in the leaves treated with ZT^{70}PU^{30} or ZnSO$_4$·6H$_2$O fertilizer, as leaves were sprayed with the same amounts of Zn (SOM-5); significative higher amount of soluble Zn was recorded in leaves treated with ZnSO$_4$·6H$_2$O compared to those treated with ZT^{70}PU^{30} (PRE rain columns in Fig. 6B), which is possibly indicative of faster availability to the plant. On the other hand, ZT^{70}PU^{30} showed a significantly better tolerance to the rain leaching, as evidenced by the higher Zn residuality, both total and soluble forms (POST rain columns in Fig. 6A and B, compared to ZnSO$_4$·6H$_2$O. This positive effect is plausibly due to the role of active ZT and PU particles, i.e., zeolitic species, in enhancing the permanence of Zn on leaves compared to the more mobile ZnSO$_4$·6H$_2$O. The increased persistence is also correlated to the physical interaction between lithoid particles of the formulation and the rough morphology of the leaf surface, which facilitates its adhesion, a feature already observed in plants treated with natural zeolitized tuffs [138]. In other word, ZT^{70}PU^{30} not only act as a carrier for Zn, but also as a holder for its residence on leaves.

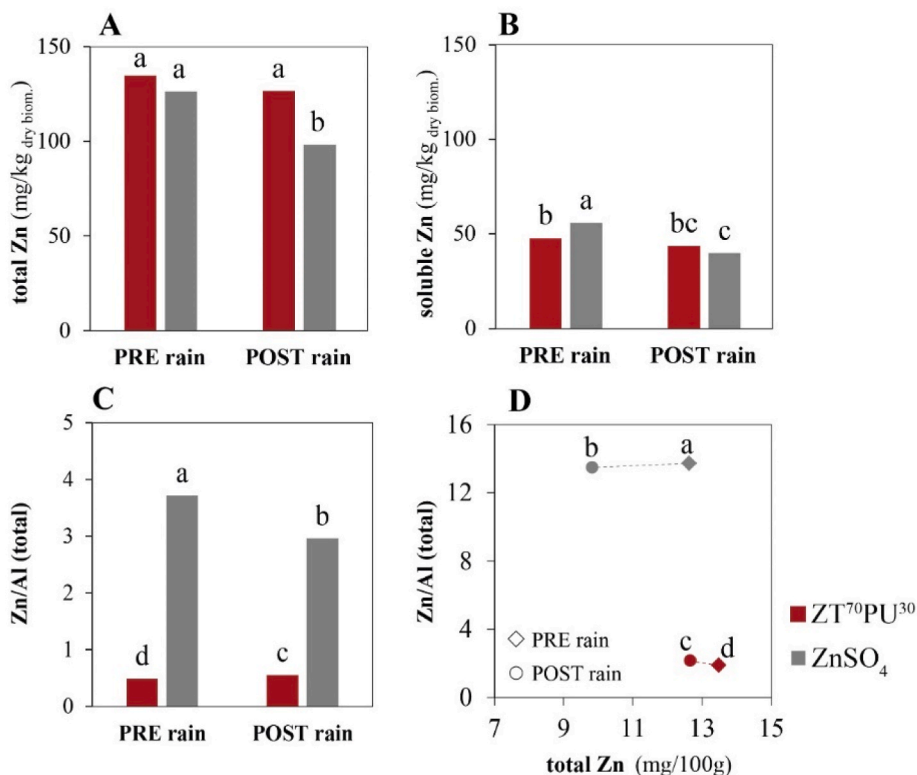Being zeolites alumo–silicates, the Zn/Al ratio could be indicative of

Fig. 6. Zn concentration on leaves and residence time before and after a simulated rain event. A) total Zn (mg/kg dry biomass); B) soluble Zn; C) Zn/Al ratio; D) total Zn vs Zn/Al plot. Two conditions are significantly different if no letter (i.e., a, b, c, d) is in common, as resulted from ANOVA and Tukey's HSD tests.

the permanence of $ZT^{70}PU^{30}$ on plant leaves (Fig. 6C and D). Indeed, the Zn/Al ratio decreases in $ZnSO_4 \cdot 6H_2O$ treated leaves after the rain event, whereas in $ZT^{70}PU^{30}$ it significantly increased, suggesting that the rain event did not much affect the persistence of mineral particles on leaves (Fig. 6C), and the capacity of zeolites in providing Zn in bioaccessible form (Zn^{2+}) was maintained more efficiently than with conventional $ZnSO_4 \cdot 6H_2O$ (Fig. 6D).

3.6. Preliminary cost outlook

Reimplementing PU and LA by-products is generally limited by their small grain size (often <3 mm). In addition, both are marked by very high operating costs, up to 1.20 €/m^3. Therefore, PU and LA by-products are mostly reused for quarry restoration, with additional costs for transportation. Alternatively, according to current Italian [139,140] and European [141] laws, quarry by-products can be stored in areas within the quarry's jurisdiction, authorized as internal landfills, and a fee must be paid if they are resold.

Although there are no industrial plants dedicated to produce the $ZT^{70}PU^{30}$, an estimate of the production cost could be obtained considering the cost of producing atomized mixtures in ceramic tile industry. The latter materials, in fact, are produced using wet grinding plants into which any geomaterial (including zeolitized tuffs) can be placed in addition to water and a soluble salt (in this case, $ZnSO_4 \cdot 6H_2O$). Given current energy and material costs, the production of a formulation consisting of 100 % ZT exchanged with Zn^{2+} is estimated at about 2.70 €/kg ($\pm$0.25 €/kg depending on the production capacity of the grinding plant). Replacing up to 30 wt% of ZT with PU ($ZT^{70}PU^{30}$) would result in savings of about 5 % of the total, but without considering the environmental benefit and fees no longer due for storage of PU by-product. These estimates, although preliminary, would allow $ZT^{70}PU^{30}$ to be placed in the current market with sale prices similar, or even lower, to those of other conventional Zn fertilizers.

4. Conclusions

Zn plant deficiency relates with plant disease, human dietary deficit and health issues. Therefore, providing Zn to crops in case of inadequate plant uptake from the soil is necessary. Zn fertilizers are however generally associated with low efficiency. A new foliar fertilizer formulation based on natural geomaterials rich in zeolites was proposed here, with the aim of meeting both the demand for efficient Zn-based plant nutrition and the disposal of problematic quarry by-products.

The best formulation, with unreduced properties respect to pure ZT, comprised 70 wt% of ZT and 30 wt% of pumice scraps. This formulation, for the same amount of Zn used, sprayed on plant of *Vitis vinifera* showed slower releasing properties and significative adhesion on leaves, proving better residence than traditional $ZnSO_4 \cdot 6H_2O$ fertilizer to rain leaching.

From the perspective of economic viability, net of environmental benefits, preliminary cost estimates suggest that $ZT^{70}PU^{30}$ can be placed in the market with competitive sales prices. Although possibly side effects are expected to be less than those experienced with conventional fertilizers, medium-to-large-scale agronomic assays will be needed before trade to demonstrate its true efficacy, absence of phytotoxicity and medium- and long-term impacts on (micro)organisms. Similarly, a comparison with other slow-release foliar fertilizers (e.g., coated/encapsulated/chelated Zn compounds) is necessary both in terms of efficacy and cost-effectiveness.

Assuming an ever-increasing demand for Zn-based fertilizers, the development of methodologies for recovering and reusing Zn from wastewater could be an additional challenge for circularity which could nicely match with the outcome of this research.

Funding

CRediT authorship contribution statement

Declaration of competing interest

Data availability

Data will be made available on request.

Acknowledgements

Appendix A. Supplementary data

Supplementary data to this article can be found online at https://doi.org/10.1016/j.micromeso.2024.113290.

References

[1] R.A. Al Dwairi, A.E. Al-Rawajfeh, Recent patents of natural zeolites applications in environment, agriculture and pharmaceutical industry, Recent Pat, Chem. Eng. 5 (2012) 20–27, https://doi.org/10.2174/1874478811205010020.

[2] I. Kithinji Kinoti, J. Ogunah, C. Muturia M'Thiruaine, J.M. Marangu, Adsorption of heavy metals in contaminated water using zeolite derived from agro-wastes and clays: a review, J. Chem. 2022 (2022) 1–25, https://doi.org/10.1155/2022/4250299.

[3] M. Mishra, S.K. Jain, Properties and applications of zeolites: a Review, Proc. Natl. Acad. Sci. India B Biol. Sci. 81 (2011) 250–259.

[4] D.Z. Rahman, J. Vijayaraghavan, J. Thivya, A comprehensive review on zinc(II) sequestration from wastewater using various natural/modified low-cost agrowaste sorbents, Biomass Convers. Biorefinery 13 (2023) 5469–5499, https://doi.org/10.1007/s13399-021-01822-1.

[5] E.I. Ugwu, A. Othmani, C.C. Nnaji, A review on zeolites as cost-effective adsorbents for removal of heavy metals from aqueous environment, Int. J. Environ. Sci. Technol. 19 (2022) 8061–8084, https://doi.org/10.1007/s13762-021-03560-3.

[6] A.A. Zorpas, J.N. Pedreño, M.B.A. Candel, Heavy metal treatment and removal using natural zeolites from sewage sludge, compost, and agricultural soils: a review, Arabian J. Geosci. 14 (2021) 1098, https://doi.org/10.1007/s12517-021-07443-2.

[7] J. Adinehvand, A. Shokuhi Rad, A.S. Tehrani, Acid-treated zeolite (clinoptilolite) and its potential to zinc removal from water sample, Int. J. Environ. Sci. Technol. 13 (2016) 2705–2712, https://doi.org/10.1007/s13762-016-1105-1.

[8] E.G. Filatova, Y.N. Pozhidaev, Removal of zinc(II) ions from wastewater using natural zeolites, IOP Conf. Ser. Earth Environ. Sci. 666 (2021) 042034, https://doi.org/10.1088/1755-1315/666/4/042034.

[9] S. Malamis, E. Katsou, A review on zinc and nickel adsorption on natural and modified zeolite, bentonite and vermiculite: examination of process parameters, kinetics and isotherms, J. Hazard Mater. 252–253 (2013) 428–461, https://doi.org/10.1016/J.JHAZMAT.2013.03.024.

[10] J. Perić, M. Trgo, N. Vukojević Medvedović, Removal of zinc, copper and lead by natural zeolite—a comparison of adsorption isotherms, Water Res. 38 (2004) 1893–1899, https://doi.org/10.1016/j.watres.2003.12.035.

[11] L. Morrone, L. Neri, O. Facini, G. Galamini, G. Ferretti, A. Rotondi, Influence of chabazite zeolite foliar applications used for olive fruit fly control on volatile organic compound emission, photosynthesis, and quality of extra virgin olive oil, Plants 13 (2024) 698, https://doi.org/10.3390/plants13050698.

[12] V. Inglezakis, A. Zorpas (Eds.), Handbook of Natural Zeolites, Bentham Science Publishers, 2012, https://doi.org/10.2174/97816080526151120101.

[13] A. Mahler (Ed.), Zeolites: Advances in Research and Applications, Nova Science Publishers, New York, 2020.

[14] F.A. Mumpton (Ed.), Mineralogy and Geology of Natural Zeolites, De Gruyter, Place of publication not identified, 2019.

[15] D.L. Bish, D.W. Ming (Eds.), Natural Zeolites: Occurrence, Properties, Applications, Mineralogical Society of America, Washington, DC, 2001.

[16] T. Campisi, F. Abbondanzi, B. Faccini, D. Di Giuseppe, D. Malferrari, M. Coltorti, A. Laurora, E. Passaglia, Ammonium-charged zeolitite effects on crop growth and nutrient leaching: greenhouse experiments on maize (Zea mays), Catena 140 (2016) 66–76, https://doi.org/10.1016/j.catena.2016.01.019.

[17] E. Cataldo, L. Salvi, F. Paoli, M. Fucile, G. Masciandaro, D. Manzi, C.M. Masini, G. B. Mattii, Application of zeolites in agriculture and other potential uses: a review, Agronomy 11 (2021), https://doi.org/10.3390/agronomy11081547.

[18] N. Eroglu, M. Emekci, C.G. Athanassiou, Applications of natural zeolites on agriculture and food production, J. Sci. Food Agric. 97 (2017) 3487–3499, https://doi.org/10.1002/jsfa.8312.

[19] G. Ferretti, G. Galamini, V. Medoro, B. Faccini, Amount and speciation of N leached from a sandy soil fertilized with urea, liquid digestate, struvite and NH4-enriched chabazite zeolite-tuff, Soil Use Manag. 39 (2023) 456–473, https://doi.org/10.1111/sum.12855.

[20] G. Galamini, G. Ferretti, C. Rosinger, S. Huber, V. Medoro, A. Mentler, E. Díaz-Pinés, M. Gorfer, B. Faccini, K.M. Keiblinger, Recycling nitrogen from liquid digestate via novel reactive struvite and zeolite minerals to mitigate agricultural pollution, Chemosphere 317 (2023) 137881, https://doi.org/10.1016/J.CHEMOSPHERE.2023.137881.

[21] Z. Ghasemi, I. Sourinejad, H. Kazemian, S. Rohani, Application of zeolites in aquaculture industry: a review, Rev. Aquacult. 10 (2018) 75–95, https://doi.org/10.1111/raq.12148.

[22] R. Jarosz, J. Szerement, K. Gondek, M. Mierzwa-Hersztek, The use of zeolites as an addition to fertilisers – a review, Catena 213 (2022), https://doi.org/10.1016/j.catena.2022.106125.

[23] D. Malferrari, A. Laurora, M.F. Brigatti, D. Di Giuseppe, B. Faccini, M. Coltorti, A time- and cost-saving method to check the point-to-point distribution of soil improvers, J. Plant Nutr. Soil Sci. (2021), https://doi.org/10.1002/jpln.202000409.

[24] D. Malferrari, A. Laurora, M.F. Brigatti, M. Coltorti, D. Di Giuseppe, B. Faccini, E. Passaglia, M.G. Vezzalini, Open-field experimentation of an innovative and integrated zeolitite cycle: project definition and material characterization, Rendiconti Lincei 24 (2013) 141–150, https://doi.org/10.1007/s12210-013-0235-3.

[25] V. Medoro, G. Ferretti, G. Galamini, A. Rotondi, L. Morrone, B. Faccini, M. Coltorti, Reducing nitrogen fertilization in olive growing by the use of natural chabazite-zeolitite as soil improver, Land 11 (2022) 1471, https://doi.org/10.3390/LAND11091471, 1471 11 (2022.

[26] B. Faccini, D. Di Giuseppe, D. Malferrari, M. Coltorti, F. Abbondanzi, T. Campisi, A. Laurora, E. Passaglia, Ammonium-exchanged zeolitite preparation for agricultural uses: from laboratory tests to large-scale application in ZeoLIFE project prototype, Period, Mineral. 84 (2015) 303–321, https://doi.org/10.2451/2015PM0015.

[27] A. Lateef, R. Nazir, N. Jamil, S. Alam, R. Shah, M.N. Khan, M. Saleem, Synthesis and characterization of zeolite based nano–composite: an environment friendly slow release fertilizer, Microporous Mesoporous Mater. 232 (2016) 174–183, https://doi.org/10.1016/j.micromeso.2016.06.020.

[28] G. Ferretti, M. Alberghini, G. Galamini, V. Medoro, B. Faccini, S. Balzan, M. Coltorti, Exploring the combined effects of different nitrogen sources and chabazite zeolite-tuff on nitrogen dynamics in an acidic sandy-loam soil, Soil Syst 8 (2024) 16, https://doi.org/10.3390/soilsystems8010016.

[29] C. Banik, S. Bakshi, D.S. Andersen, D.A. Laird, R.G. Smith, R.C. Brown, The role of biochar and zeolite in enhancing nitrogen and phosphorus recovery: a sustainable manure management technology, Chem. Eng. J. 456 (2023) 141003, https://doi.org/10.1016/j.cej.2022.141003.

[30] M. Eslami, R. Khorassani, M. Coltorti, D. Malferrari, B. Faccini, G. Ferretti, D. Di Giuseppe, A. Fotovat, A. Halajnia, Leaching behaviour of a sandy soil amended with natural and NH4+ and K+ saturated clinoptilolite and chabazite, Arch. Agron Soil Sci. 64 (2018) 1142–1151, https://doi.org/10.1080/03650340.2017.1414944.

[31] G. Galamini, G. Ferretti, V. Medoro, N. Tescaro, B. Faccini, M. Coltorti, Isotherms, kinetics, and thermodynamics of NH4+ adsorption in raw liquid manure by using natural chabazite zeolite-rich tuff, Water 12 (2020) 2944, https://doi.org/10.3390/w12102944.

[32] S. Montalvo, C. Huiliñir, A. Castillo, J. Pagés-Díaz, L. Guerrero, Carbon, nitrogen and phosphorus recovery from liquid swine wastes: a review, J. Chem. Technol. Biotechnol. 95 (2020) 2335–2347, https://doi.org/10.1002/jctb.6336.

[33] A. Santoso, D.C. Lukito, E.H. Sanjaya, S. Sumari, A.R. Wijaya, D.E. Putri, M. R. Asrori, The effect of starter on biogas production of anaerobic digestion of cow manure using active zeolite, in: Malang, Indonesia, 2023 070011, https://doi.org/10.1063/5.0112760.

[34] V.A. Tzanakakis, N. Monokrousos, T. Chatzistathis, Effects of clinoptilolite zeolite and vermiculite on nitrification and nitrogen and phosphorus acquiring enzymes in a nitrogen applied agricultural soil, J. Soil Sci. Plant Nutr. 21 (2021) 2791–2802, https://doi.org/10.1007/s42729-021-00566-1.

[35] J. Viaene, N. Peiren, D. Vandamme, A. Lataf, A. Cuypers, M. Jozefczak, B. Vandecasteele, Biochar amendment to cattle slurry reduces NH3 emissions during storage without risk of higher NH3 emissions after soil application of the solid fraction, Waste Manag. 167 (2023) 39–45, https://doi.org/10.1016/j.wasman.2023.05.023.

[36] F. Calzarano, L. Seghetti, G. Pagnani, S. Di Marco, Italian zeolites in the control of grey mould and sour rot and their effect on leaf reflectance, grape and wine, Agric. For. 10 (2020) 580, https://doi.org/10.3390/AGRICULTURE10120580, 580 10 (2020.

[37] F. Calzarano, G. Valentini, G. Arfelli, L. Seghetti, A.C. Manetta, E.G. Metruccio, S. Di Marco, Activity of Italian natural chabasite-rich zeolites against grey mould, sour rot and grapevine moth, and effects on grape and wine composition, Phytopathol. Mediterr. 58 (2019) 309–323, https://doi.org/10.14601/Phytopathol_Mediter-10618.

[38] E. Cataldo, M. Fucile, G.B. Mattii, Leaf eco-physiological profile and berries technological traits on potted Vitis vinifera L. Cv pinot noir subordinated to zeolite treatments under drought stress, Plants 11 (2022) 1735, https://doi.org/10.3390/plants11131735.

[39] C. De Smedt, E. Someus, P. Spanoghe, Potential and actual uses of zeolites in crop protection, Pest Manag. Sci. 71 (2015) 1355–1367, https://doi.org/10.1002/ps.3999.

[40] D.M. Glenn, G. Puterka, Particle film technology: an overview of history, concepts and impact in horticulture, Acta Hortic. 636 (2004) 509–511, https://doi.org/10.17660/ActaHortic.2004.636.63.

[41] D. Malferrari, S. Poppi, Product for defending and feeding plants and respective preparation method and use, EP3238541 (A1), https://worldwide.espacenet.com/publicationDetails/biblio?FT=D&date=20171101&DB=&locale=en_EP&CC=EP&NR=3238541A1&KC=A1&ND=1, 2017. (Accessed 3 January 2023).

[42] D.G. Petoumenou, Enhancing yield and physiological performance by foliar applications of chemically inert mineral particles in a rainfed vineyard under mediterranean conditions, Plants 12 (2023) 1444, https://doi.org/10.3390/plants12071444.

[43] A. Rotondi, G. Bertazza, B. Faccini, G. Ferretti, L. Morrone, Effect of different foliar particle films (kaolin and zeolitite) on chemical and sensory properties of olive oil, Agronomy 12 (2022) 3088, https://doi.org/10.3390/agronomy12123088.

[44] N. Shahsavari, A. Dadrasnia, Effect of zeolites and zinc on the physiological characteristics of canola under late-season drought stress, Commun. Soil Sci. Plant Anal. 47 (2016) 2077–2087, https://doi.org/10.1080/00103624.2016.1228940.

[45] R. Panek, M. Medykowska, M. Wiśniewska, K. Szewczuk-Karpisz, K. Jędruchniewicz, M. Franus, Simultaneous removal of Pb2+ and Zn2+ heavy metals using fly ash Na-X zeolite and its carbon Na-X(C) composite, Materials 14 (2021) 2832, https://doi.org/10.3390/ma14112832.

[46] J. Szerement, A. Szatanik-Kloc, R. Jarosz, T. Bajda, M. Mierzwa-Hersztek, Contemporary applications of natural and synthetic zeolites from fly ash in agriculture and environmental protection, J. Clean. Prod. 311 (2021) 127461, https://doi.org/10.1016/j.jclepro.2021.127461.

[47] X. Chen, P. Zhang, Y. Wang, W. Peng, Z. Ren, Y. Li, B. Chu, Q. Zhu, Research progress on synthesis of zeolites from coal fly ash and environmental applications, Front. Environ. Sci. Eng. 17 (2023) 149, https://doi.org/10.1007/s11783-023-1749-2.

[48] F.A. Mumpton, La roca magica: uses of natural zeolites in agriculture and industry, Proc. Natl. Acad. Sci. U.S.A. 96 (1999) 3463–3470, https://doi.org/10.1073/pnas.96.7.3463.

[49] G.U.156-104, Modifica degli allegati 2, 6 e 7 del DGLS 75 del 29 aprile 2010, 2015.

[50] M. Tayebi-Khorami, M. Edraki, G. Corder, A. Golev, Re-thinking mining waste through an integrative approach led by circular economy aspirations, Minerals 9 (2019) 286, https://doi.org/10.3390/min9050286.

[51] M. Yuvaraj, K.S. Subramanian, Development of slow release Zn fertilizer using nano-zeolite as carrier, J. Plant Nutr. 41 (2018) 311–320, https://doi.org/10.1080/01904167.2017.1381729.

[52] M. Senila, O. Cadar, L. Senila, B.S. Angyus, Simulated bioavailability of heavy metals (Cd, Cr, Cu, Pb, Zn) in contaminated soil amended with natural zeolite using diffusive gradients in thin-films (DGT) technique, Agriculture 12 (2022) 321, https://doi.org/10.3390/agriculture12030321.

[53] G. Garau, P. Castaldi, L. Santona, P. Deiana, P. Melis, Influence of red mud, zeolite and lime on heavy metal immobilization, culturable heterotrophic microbial populations and enzyme activities in a contaminated soil, Geoderma 142 (2007) 47–57, https://doi.org/10.1016/j.geoderma.2007.07.011.

[54] N. Roohani, R. Hurrell, R. Kelishadi, R. Schulin, Zinc and its importance for human health: an integrative review, J. Res. Med. Sci. Off. J. Isfahan Univ. Med. Sci. 18 (2013) 144–157.

[55] R.J. Cousins, Absorption, transport, and hepatic metabolism of copper and zinc: special reference to metallothionein and ceruloplasmin, Physiol. Rev. 65 (1985) 238–309, https://doi.org/10.1152/physrev.1985.65.2.238.

[56] A.K. Baltaci, K. Yuce, R. Mogulkoc, Zinc metabolism and metallothioneins, Biol. Trace Elem. Res. 183 (2018) 22–31, https://doi.org/10.1007/s12011-017-1119-7.

[57] A. Hussain, W. Jiang, X. Wang, S. Shahid, N. Saba, M. Ahmad, A. Dar, S. U. Masood, M. Imran, A. Mustafa, Mechanistic impact of zinc deficiency in human development, Front. Nutr. 9 (2022). https://www.frontiersin.org/articles/10.3389/fnut.2022.717064. (Accessed 28 February 2024).

[58] A.M. Adamo, X. Liu, P. Mathieu, J.R. Nuttall, S. Supasai, P.I. Oteiza, Early developmental marginal zinc deficiency affects neurogenesis decreasing neuronal number and altering neuronal specification in the adult rat brain, Front. Cell. Neurosci. 13 (2019). https://www.frontiersin.org/articles/10.3389/fncel.2019.00062. (Accessed 26 April 2023).

[59] R.E. Black, L.H. Allen, Z.A. Bhutta, L.E. Caulfield, M. de Onis, M. Ezzati, C. Mathers, J. Rivera, Maternal and child undernutrition: global and regional exposures and health consequences, Lancet 371 (2008) 243–260, https://doi.org/10.1016/S0140-6736(07)61690-0.

[60] I. Cakmak, U.B. Kutman, Agronomic biofortification of cereals with zinc: a review, Eur. J. Soil Sci. 69 (2018) 172–180, https://doi.org/10.1111/ejss.12437.

[61] N.F. Krebs, L.V. Miller, K.M. Hambidge, Zinc deficiency in infants and children: a review of its complex and synergistic interactions, Paediatr. Int. Child Health 34 (2014) 279–288, https://doi.org/10.1179/2046905514Y.0000000151.

[62] B.J. Alloway, Micronutrients and crop production: an introduction, in: B. J. Alloway (Ed.), Micronutr. Defic. Glob. Crop Prod., Springer Netherlands, Dordrecht, 2008, pp. 1–39, https://doi.org/10.1007/978-1-4020-6860-7_1.

[63] Y.-M. Liu, D.-Y. Liu, Q.-Y. Zhao, W. Zhang, X.-X. Chen, S.-J. Xu, C.-Q. Zou, Zinc fractions in soils and uptake in winter wheat as affected by repeated applications of zinc fertilizer, Soil Tillage Res. 200 (2020) 104612, https://doi.org/10.1016/j.still.2020.104612.

[64] A. Moreno-Lora, A. Delgado, Factors determining Zn availability and uptake by plants in soils developed under Mediterranean climate, Geoderma 376 (2020) 114509, https://doi.org/10.1016/j.geoderma.2020.114509.

[65] N.Y. Harari, From Animals into Gods. A Brief History of Humankind, CreateSpace Independent Publishing, 2020.

[66] H. Zhang, Y. Zhao, Z. Wang, Y. Liu, Distribution characteristics, bioaccumulation and trophic transfer of heavy metals in the food web of grassland ecosystems, Chemosphere 278 (2021) 130407, https://doi.org/10.1016/j.chemosphere.2021.130407.

[67] D. Daccak, F.C. Lidon, C.C. Pessoa, I.C. Luís, A.R.F. Coelho, A.C. Marques, J. C. Ramalho, M.J. Silva, A.P. Rodrigues, M. Guerra, R.G. Leitão, P.S. Campos, I. P. Pais, J.N. Semedo, M.M. Silva, J.C. Kullberg, M. Brito, C. Galhano, P. Legoinha, M.F. Pessoa, M. Simões, F.H. Reboredo, Enrichment of grapes with zinc-efficiency of foliar fertilization with ZnSO4 and ZnO and implications on winemaking, Plants 11 (2022) 1399, https://doi.org/10.3390/plants11111399.

[68] D. Porro, D. Bertoldi, M. Bottura, S. Pedò, Evaluation of nutrient uptake on grapevine resistant cultivars, Acta Hortic. (2022) 35–42, https://doi.org/10.17660/ActaHortic.2022.1333.5.

[69] A. Sabir, G. Sari, Zinc pulverization alleviates the adverse effect of water deficit on plant growth, yield and nutrient acquisition in grapevines (Vitis vinifera L.), Sci. Hortic. 244 (2019) 61–67, https://doi.org/10.1016/j.scienta.2018.09.035.

[70] M. kazem Souri, F.Y. Sooraki, M. Moghadamyar, Growth and quality of cucumber, tomato, and green bean under foliar and soil applications of an aminochelate fertilizer, Hortic. Environ. Biotechnol. 58 (2017) 530–536, https://doi.org/10.1007/s13580-017-0349-0.

[71] C. Stanton, D. Sanders, U. Krämer, D. Podar, Zinc in plants: integrating homeostasis and biofortification, Mol. Plant 15 (2022) 65–85, https://doi.org/10.1016/j.molp.2021.12.008.

[72] C. Cabot, S. Martos, M. Llugany, B. Gallego, R. Tolrà, C. Poschenrieder, A role for zinc in plant defense against pathogens and herbivores, Front. Plant Sci. 10 (2019), https://doi.org/10.3389/fpls.2019.01171.

[73] H. Fones, C.A.R. Davis, A. Rico, F. Fang, J.A.C. Smith, G.M. Preston, Metal hyperaccumulation armors plants against disease, PLoS Pathog. 6 (2010) e1001093, https://doi.org/10.1371/journal.ppat.1001093.

[74] V. Escudero, D. Ferreira Sánchez, I. Abreu, S. Sopeña-Torres, N. Makarovsky-Saavedra, M. Bernal, U. Krämer, D. Grolimund, M. González-Guerrero, L. Jordá, Arabidopsis thaliana Zn^{2+}-efflux ATPases HMA2 and HMA4 are required for resistance to the necrotrophic fungus Plectosphaerella cucumerina BMM, J. Exp. Bot. 73 (2022) 339–350, https://doi.org/10.1093/jxb/erab400.

[75] J. Claus, A. Bohmann, A. Chavarría-Krauser, Zinc uptake and radial transport in roots of Arabidopsis thaliana: a modelling approach to understand accumulation, Ann. Bot. 112 (2013) 369, https://doi.org/10.1093/aob/mcs263.

[76] I. Cakmak, Enrichment of cereal grains with zinc: agronomic or genetic biofortification? Plant Soil 302 (2008) 1–17, https://doi.org/10.1007/s11104-007-9466-3.

[77] S.S. Dhaliwal, V. Sharma, A.K. Shukla, V. Verma, M. Kaur, Y.S. Shivay, S. Nisar, A. Gaber, M. Brestic, V. Barek, M. Skalicky, P. Ondrisik, A. Hossain, Biofortification—a frontier novel approach to enrich micronutrients in field crops

to encounter the nutritional security, Molecules 27 (2022), https://doi.org/10.3390/molecules27041340.

[78] H. El-Ramady, N. Abdalla, H. Elbasiouny, F. Elbehiry, T. Elsakhawy, A.E.-D. Omara, M. Amer, Y. Bayoumi, T.A. Shalaby, Y. Eid, M. Zia-ur- Rehman, Nano-biofortification of different crops to immune against COVID-19: a review, Ecotoxicol. Environ. Saf. 222 (2021) 112500, https://doi.org/10.1016/j.ecoenv.2021.112500.

[79] V.K. Venugopalan, R. Nath, S.C. M A, Smart fertilizers–a way ahead for sustainable agriculture, J, Plant Nutr 45 (2022) 2068–2076, https://doi.org/10.1080/01904167.2022.2046065.

[80] C.Q. Zou, Y.Q. Zhang, A. Rashid, H. Ram, E. Savasli, R.Z. Arisoy, I. Ortiz-Monasterio, S. Simunji, Z.H. Wang, V. Sohu, M. Hassan, Y. Kaya, O. Onder, O. Lungu, M.Y. Mujahid, A.K. Joshi, Y. Zelenskiy, F.S. Zhang, I. Cakmak, Biofortification of wheat with zinc through zinc fertilization in seven countries, Plant Soil 361 (2012) 119–130, https://doi.org/10.1007/s11104-012-1369-2.

[81] R. Baruah, Towards the bioavailability of zinc in agricultural soils, in: V.S. Meena (Ed.), Role Rhizospheric Microbes Soil Vol. 2 Nutr. Manag. Crop Improv., Springer, Singapore, 2018, pp. 99–136, https://doi.org/10.1007/978-981-13-0044-8_4.

[82] Y. Chen, H. Mi, Y. Zhang, G. Zhang, C. Li, Y. Ye, R. Zhang, J. Shi, Z. Li, X. Tian, Y. Wang, Impact of ZnSO4 and ZnEDTA applications on wheat Zn biofortification, soil Zn fractions and bacterial community: significance for public health and agroecological environment, Appl. Soil Ecol. 176 (2022) 104484, https://doi.org/10.1016/j.apsoil.2022.104484.

[83] M.K. Desta, M.R. Broadley, S.P. McGrath, J. Hernandez-Allica, K.L. Hassall, S. Gameda, T. Amede, S.M. Haefele, Plant available zinc is influenced by landscape position in the amhara region, Ethiopia, Plants 10 (2021) 254, https://doi.org/10.3390/plants10020254.

[84] S.S. Dhaliwal, V. Sharma, A.K. Shukla, J. Kaur, V. Verma, M. Kaur, P. Singh, A. Gaber, A. Hossain, Zinc-based mineral (ZnSO4·7H2O) and chelated (Zn-edta) fertilizers improve the productivity, quality and efficiency indices of field pea (pisum sativum l.) through biofortification, J. Trace Elem. Miner. 2 (2022) 100033, https://doi.org/10.1016/j.jtemin.2022.100033.

[85] C.L. Doolette, T.L. Read, C. Li, K.G. Scheckel, E. Donner, P.M. Kopittke, J. K. Schjoerring, E. Lombi, Foliar application of zinc sulphate and zinc EDTA to wheat leaves: differences in mobility, distribution, and speciation, J. Exp. Bot. 69 (2018) 4469–4481, https://doi.org/10.1093/jxb/ery236.

[86] M.G. Palmgren, S. Clemens, L.E. Williams, U. Krämer, S. Borg, J.K. Schjørring, D. Sanders, Zinc biofortification of cereals: problems and solutions, Trends Plant Sci. 13 (2008) 464–473, https://doi.org/10.1016/j.tplants.2008.06.005.

[87] Z. Wang, H. Wang, C. Xu, G. Lv, Z. Luo, H. Zhu, S. Wang, Q. Zhu, D. Huang, B. Li, Foliar application of Zn-edta at early filling stage to increase grain Zn and Fe, and reduce grain Cd, Pb and grain yield in rice (oryza sativa L.), Bull. Environ. Contam. Toxicol. 105 (2020) 428–432, https://doi.org/10.1007/s00128-020-02949-z.

[88] M. Xu, L. Du, M. Liu, J. Zhou, W. Pan, H. Fu, X. Zhang, Q. Ma, L. Wu, Glycine-chelated zinc rather than glycine-mixed zinc has lower foliar phytotoxicity than zinc sulfate and enhances zinc biofortification in waxy corn, Food Chem. 370 (2022) 131031, https://doi.org/10.1016/j.foodchem.2021.131031.

[89] A. Zhao, S. Yang, B. Wang, X. Tian, Y. Zhang, Effects of ZnSO$_4$ and Zn-EDTA broadcast or banded to soil on Zn bioavailability in wheat (Triticum aestivum L.) and Zn fractions in soil, Chemosphere 205 (2018) 350–360, https://doi.org/10.1016/j.chemosphere.2018.04.115.

[90] N. Putwattana, M. Kruatrachue, A. Kumsopa, P. Pokethitiyook, Evaluation of organic and inorganic amendments on maize growth and uptake of Cd and Zn from contaminated paddy soils, Int. J. Phytoremediation 17 (2015) 165–174, https://doi.org/10.1080/15226514.2013.876962.

[91] S. Ghasemi, A.H. Khoshgoftarmanesh, M. Afyuni, H. Hadadzadeh, The effectiveness of foliar applications of synthesized zinc-amino acid chelates in comparison with zinc sulfate to increase yield and grain nutritional quality of wheat, Eur. J. Agron. 45 (2013) 68–74, https://doi.org/10.1016/j.eja.2012.10.012.

[92] J. Niu, C. Liu, M. Huang, K. Liu, D. Yan, Effects of foliar fertilization: a review of current status and future perspectives, J. Soil Sci. Plant Nutr. 21 (2021) 104–118, https://doi.org/10.1007/s42729-020-00346-3.

[93] B.-G. Yu, Y.-M. Liu, X.-X. Chen, W.-Q. Cao, T.-B. Ding, C.-Q. Zou, Foliar zinc application to wheat may lessen the zinc deficiency burden in rural quzhou, China, Front. Nutr. 8 (2021). https://www.frontiersin.org/articles/10.3389/fnut.2021.697817. (Accessed 27 April 2023).

[94] B.S. Haslett, R.J. Reid, Z. Rengel, Zinc mobility in wheat: uptake and distribution of zinc applied to leaves or roots, Ann. Bot. 87 (2001) 379–386, https://doi.org/10.1006/anbo.2000.1349.

[95] B. Erenoglu, M. Nikolic, V. Römheld, I. Cakmak, Uptake and transport of foliar applied zinc (65Zn) in bread and durum wheat cultivars differing in zinc efficiency, Plant Soil 241 (2002) 251–257, https://doi.org/10.1023/A:1016148925918.

[96] C.L. Doolette, T.L. Read, N.R. Howell, T. Cresswell, E. Lombi, Zinc from foliar-applied nanoparticle fertiliser is translocated to wheat grain: a 65Zn radiolabelled translocation study comparing conventional and novel foliar fertilisers, Sci. Total Environ. 749 (2020) 142369, https://doi.org/10.1016/j.scitotenv.2020.142369.

[97] I. Cakmak, U.B. Kutman, Agronomic biofortification of cereals with zinc: a review, Eur. J. Soil Sci. 69 (2018) 172–180, https://doi.org/10.1111/ejss.12437.

[98] V. Fernandez, P.H. Brown, From plant surface to plant metabolism: the uncertain fate of foliar-applied nutrients, Front. Plant Sci. 4 (2013). https://www.frontiersin.org/articles/10.3389/fpls.2013.00289. (Accessed 9 May 2023).

[99] A. Shaviv, Advances in controlled-release fertilizers, Adv. Agron. 71 (2001) 1–49, https://doi.org/10.1016/S0065-2113(01)71011-5.

[100] M.L. Fercia, R. Lonis, R. Peretti, A. Sau, A. Serci, A. Zucca, Mineralogical characteristics and cationic exchange properties of a zeolite mineral from romana, NW Sardinia, Italy, Resour. Geol. 59 (2009) 15–24, https://doi.org/10.1111/j.1751-3928.2008.00077.x.

[101] E. Passaglia, A. Laurora, NH4 exchange in chabazite, heulandite–clinoptilolite, and phillipsite, Rendiconti Lincei 24 (2013) 369–376, https://doi.org/10.1007/s12210-013-0257-x.

[102] E. Pérez-Botella, S. Valencia, F. Rey, Zeolites in adsorption processes: state of the art and future prospects, Chem. Rev. 122 (2022) 17647–17695, https://doi.org/10.1021/acs.chemrev.2c00140.

[103] E. Castellini, D. Malferrari, F. Bernini, M.F. Brigatti, G.R. Castro, L. Medici, A. Mucci, M. Borsari, Baseline studies of the clay minerals society source clay montmorillonite stx-1b, Clay Clay Miner. 65 (2017) 220–233, https://doi.org/10.1346/CCMN.2017.064065.

[104] A.F. Gualtieri, G.D. Gatta, R. Arletti, G. Artioli, P. Ballirano, G. Cruciani, A. Guagliardi, D. Malferrari, N. Masciocchi, P. Scardi, Quantitative phase analysis using the Rietveld method: towards a procedure for checking the reliability and quality of the results, Period. Mineral. 88 (2019) 147–151, https://doi.org/10.2451/2019PM870.

[105] F. Altimari, I. Lancellotti, C. Leonelli, F. Andreola, H. Elsayed, E. Bernardo, L. Barbieri, Green materials for construction industry from Italian volcanic quarry scraps, Mater. Lett. 333 (2023) 133615, https://doi.org/10.1016/j.matlet.2022.133615.

[106] L. Barbieri, F. Altimari, F. Andreola, B. Maggi, I. Lancellotti, Characterization of volcano-sedimentary rocks and related scraps for design of sustainable materials, Materials 16 (2023) 3408, https://doi.org/10.3390/ma16093408.

[107] F. Altimari, F. Andreola, P.P. Benassi, I. Lancellotti, L. Barbieri, Pumice and lapillus scraps: new national environmental-friendly chance for the production of ceramic tiles, Ceram. Int. 49 (2023) 38743–38753, https://doi.org/10.1016/j.ceramint.2023.09.211.

[108] R. Wang, K. Mi, X. Yuan, J. Chen, J. Pu, X. Shi, Y. Yang, H. Zhang, H. Zhang, Zinc oxide nanoparticles foliar application effectively enhanced zinc and aroma content in rice (oryza sativa L.) grains, Rice 16 (2023) 36, https://doi.org/10.1186/s12284-023-00653-0.

[109] X. Wei, Y. Zhang, X. Song, L. Zhao, Q. Zhao, T. Chen, K. Lu, Z. Zhu, S. Huang, C. Wang, Silicon and zinc fertilizer application improves grain quality and aroma in the japonica rice variety nanjing 46, Foods 13 (2024) 152, https://doi.org/10.3390/foods13010152.

[110] A. Bahmanzadegan, H. Tavallali, V. Tavallali, M.A. Karimi, Variations in biochemical characteristics of Zataria multiflora in response to foliar application of zinc nano complex formed on pomace extract of Punica granatum, Ind. Crops Prod. 187 (2022) 115369, https://doi.org/10.1016/j.indcrop.2022.115369.

[111] G.E. Likens, R.F. Wright, J.N. Galloway, T.J. Butler, Acid rain, Sci. Am. 241 (1979) 43–51.

[112] R core team, R Studio. https://www.r-project.org, 2019.

[113] W.N. Venables, B.D. Ripley, Modern Applied Statistics with S, Fourth edition, New York, 2002. https://www.stats.ox.ac.uk/pub/MASS4/.

[114] F. Mendiburu, M. Yaseen, Agricolae: statistical procedures for agricultural research, R package version 1.4.0 (2020). https://cran.r-project.org/package=agricolae.

[115] I.C. Madsen, N.V.Y. Scarlett, A. Kern, Description and survey of methodologies for the determination of amorphous content via X-ray powder diffraction, Z. Kristallogr. 226 (2011) 944–955, https://doi.org/10.1524/zkri.2011.1437.

[116] H.D. Young, Statistical Treatment of Experimental Data, McGraw-Hill Book Company, New York, 1962.

[117] V.J. Inglezakis, The concept of "capacity" in zeolite ion-exchange systems, J. Colloid Interface Sci. 281 (2005) 68–79, https://doi.org/10.1016/J.JCIS.2004.08.082.

[118] O. Ergürhan, B. Erdoğan, Effect of calcination after NH4NO3 modification of natural clinoptilolite on the structural and textural properties, Russ. J. Phys. Chem. A 97 (2023) 3136–3142, https://doi.org/10.1134/S0036024423130083.

[119] A. Nikolov, H. Nugteren, I. Rostovsky, Optimization of geopolymers based on natural zeolite clinoptilolite by calcination and use of aluminate activators, Construct. Build. Mater. 243 (2020) 118257, https://doi.org/10.1016/j.conbuildmat.2020.118257.

[120] Z. Tisler, J. Horacek, J. Safar, R. Velvarska, L. Peliskova, J. Kocik, Y. Gherib, K. Marklova, R. Bulanek, D. Kubicka, Clinoptilolite foams prepared by alkali activation of natural zeolite and their post-synthesis modifications, Microporous Mesoporous Mater. 282 (2019) 169–178, https://doi.org/10.1016/j.micromeso.2019.03.029.

[121] Y. Liu, S. Zhao, X. Qiu, Y. Meng, H. Wang, S. Zhou, Q. Qiao, C. Yan, Clinoptilolite based zeolite-geopolymer hybrid foams: potential application as low-cost sorbents for heavy metals, J. Environ. Manag. 330 (2023) 117167, https://doi.org/10.1016/j.jenvman.2022.117167.

[122] J. Gorimbo, B. Taenzana, A.A. Muleja, A.T. Kuvarega, L.L. Jewell, Adsorption of cadmium, nickel and lead ions: equilibrium, kinetic and selectivity studies on modified clinoptilolites from the USA and RSA, Environ. Sci. Pollut. Res. 25 (2018) 30962–30978, https://doi.org/10.1007/s11356-018-2992-0.

[123] M. de'Gennaro, A. Langella, Italian zeolitized rocks of technological interest, Miner. Deposita 31 (1996) 452–472, https://doi.org/10.1007/BF00196127.

[124] N. Kabdaşlı, I. Arslan-Alaton, T. Olmez-Hanci, O. Tunay, Electrocoagulation applications for industrial wastewaters: a critical review, Environ. Technol. Rev. 1 (2012) 2–45, https://doi.org/10.1080/21622515.2012.715390.

[125] K.S. Larsen, D.S. Auld, Carboxypeptidase A: mechanism of zinc inhibition, Biochemistry 28 (1989) 9620–9625, https://doi.org/10.1021/bi00451a012.

[126] M.E. McMahon, R.J. Santucci, J.R. Scully, Advanced chemical stability diagrams to predict the formation of complex zinc compounds in a chloride environment, RSC Adv. 9 (2019) 19905–19916, https://doi.org/10.1039/C9RA00228F.

[127] A. Langella, M. Pansini, P. Cappelletti, B. de Gennaro, M. de' Gennaro, C. Colella, NH_4^+, Cu^{2+}, Zn^{2+}, Cd^{2+} and Pb^{2+} exchange for Na^+ in a sedimentary clinoptilolite, North Sardinia, Italy, Microporous Mesoporous Mater. 37 (2000) 337–343, https://doi.org/10.1016/S1387-1811(99)00276-0.

[128] J.P. Simonin, On the comparison of pseudo-first order and pseudo-second order rate laws in the modeling of adsorption kinetics, Chem. Eng. J. 300 (2016) 254–263, https://doi.org/10.1016/j.cej.2016.04.079.

[129] J. Li, M. Gao, W. Yan, J. Yu, Regulation of the Si/Al ratios and Al distributions of zeolites and their impact on properties, Chem. Sci. 14 (2023) 1935–1959, https://doi.org/10.1039/D2SC06010H.

[130] W.J. Weber, J.C. Morris, Kinetics of adsorption on carbon from solution, J. Sanit. Eng. Div. 89 (1963) 31–60.

[131] Y.S. Ho, G. McKay, Pseudo-second order model for sorption processes, Process Biochem. 34 (1999) 451–465, https://doi.org/10.1016/S0032-9592(98)00112-5.

[132] Y. Xiao, J. Azaiez, J.M. Hill, Erroneous application of pseudo-second-order adsorption kinetics model: ignored assumptions and spurious correlations, Ind. Eng. Chem. Res. 57 (2018) 2705–2709, https://doi.org/10.1021/acs.iecr.7b04724.

[133] I. Nuić, M. Trgo, J. Perić, N. Vukojević Medvidović, Analysis of breakthrough curves of Pb and Zn sorption from binary solutions on natural clinoptilolite, Microporous Mesoporous Mater. 167 (2013) 55–61, https://doi.org/10.1016/j.micromeso.2012.04.037.

[134] S. Wasielewski, E. Rott, R. Minke, H. Steinmetz, Evaluation of different clinoptilolite zeolites as adsorbent for ammonium removal from highly concentrated synthetic wastewater, Water 10 (2018) 584, https://doi.org/10.3390/w10050584.

[135] F.C. Wu, R.L. Tseng, R.S. Juang, Initial behavior of intraparticle diffusion model used in the description of adsorption kinetics, Chem. Eng. J. 153 (2009) 1–8, https://doi.org/10.1016/j.cej.2009.04.042.

[136] G. Gottardi, E. Galli, Natural Zeolites, Springer-Verlag, Berlin Heidelberg NewYork Tokio, 1985.

[137] E. Passaglia, E. Galli, Natural zeolites: mineralogy and applications, Eur. J. Mineral 3 (1991) 637–640, https://doi.org/10.1127/ejm/3/4/0637.

[138] A. Rotondi, L. Morrone, O. Facini, B. Faccini, G. Ferretti, M. Coltorti, Distinct particle films impacts on olive leaf optical properties and plant physiology, Foods Basel Switz 10 (2021), https://doi.org/10.3390/FOODS10061291.

[139] DL 152/2006. https://www.normattiva.it/uri-res/N2Ls?urn:nir:stato:decreto.legislativo:2006-04-03;152, 2006. (Accessed 21 December 2023).

[140] Dpr 120/2017. https://www.normattiva.it/uri-res/N2Ls?urn:nir:stato:decreto.del.presidente.della.repubblica:2017-06-13;120!vig=, 2017. (Accessed 21 December 2023).

[141] 2008/98/EC, Directive 2008/98/EC of the European Parliament and of the Council of 19 November 2008 on Waste and Repealing Certain Directives (Text with EEA Relevance), 2008. http://data.europa.eu/eli/dir/2008/98/oj/eng. (Accessed 21 December 2023).